2017

Impact of a monolithic silicon detector operating in transmission mode on clinical photon beams

Kananan Utitsarn
University of Wollongong, ku566@uowmail.edu.au

Z A. Alrowaili
Aljouf University, zaa931@uowmail.edu.au

Nauljun Stansook
University of Wollongong, ns938@uowmail.edu.au

Marco Petasecca
University of Wollongong, marcop@uow.edu.au

Martin G. Carolan
University of Wollongong, mcarolan@uow.edu.au

See next page for additional authors

Impact of a monolithic silicon detector operating in transmission mode on clinical photon beams

Abstract

Purpose

To investigate the effect on surface dose, as a function of different field sizes and distances from the solid water phantom to transmission detector (D_{sd}), of using the monolithic silicon detector MP512T in transmission mode.

Methods

The influence of operating the MP512T in transmission mode on the surface dose of a phantom for SSD 100cm was evaluated by using a Markus IC. The MP512T was fixed to an adjustable stand holder and was positioned at different D_{sd}, ranging from 0.3 to 24 cm. For each D_{sd}, measurements were carried out for irradiation field sizes of 5 × 5cm^2, 8 × 8 cm^2 and 10 × 10 cm^2. Measurements were obtained under two different operational setups, (i) with the MP512T face-up and (ii) with the MP512T face-down. In addition, the transmission factors for the MP512T and the printed circuit board were only evaluated using a Farmer IC.

Results

For all D_{sd} and all field sizes, the MP512T led to the surface dose increasing by less than 25% when in the beam. For D_{sd} >18 cm the surface dose increase is less than 5%, and negligible for field size 5 × 5 cm^2. The difference in the surface dose perturbation for the MP512T operating face up or operating face down is negligible (sd and field sizes.

Conclusion

The study demonstrated that positioning the MP512T in air between the Linac head and the phantom produced negligible perturbation of the surface dose for D_{sd} >18 cm, and was completely transparent for 6 MV photon beams.

Disciplines

Engineering | Science and Technology Studies

Publication Details

Utitsarn, K., Alrowaili, Z. A., Stansook, N., Petasecca, M., Carolan, M., Perevertaylo, V. L., Lerch, M. & Rosenfeld, A. (2017). Impact of a monolithic silicon detector operating in transmission mode on clinical photon beams. Physica Medica: an international journal devoted to the applications of physics to medicine and biology, 43 114-119.

Authors

Kananan Utitsarn, Z A. Alrowaili, Nauljun Stansook, Marco Petasecca, Martin G. Carolan, Vladimir Perevertaylo, Michael L. F Lerch, and Anatoly B. Rosenfeld

Impact of a monolithic silicon detector operating in transmission mode on clinical photon beams

Kananan Utitsarn[1], Nauljun Stansook[1], Ziyad Alrowaili[1], Marco Petasecca[1], Martin Carolan[2], Michael Lerch[1] and Anatoly Rosenfeld[1]

[1] Centre for Medical Radiation Physics, University of Wollongong, Australia.

[2] Illawarra Cancer Care Centre, Wollongong Hospital, Australia.

Abstract

Purpose: To investigate the effect on surface dose, as a function of different field sizes and distances from the solid water phantom to transmission detector (D_{sd}), of using the monolithic silicon detector MP512T in transmission mode.

Methods: The influence of operating the MP512T in transmission mode on the surface dose of a phantom for SSD 100cm was evaluated by using a Markus IC. The MP512T was fixed to an adjustable stand holder and was positioned at different D_{sd}, ranging from 0.3-24cm. For each D_{sd}, measurements were carried out for irradiation field sizes of 5x5cm^2,8x8cm^2 and 10x10cm^2. Measurements were obtained under two different operational setups, (i)with the MP512T face-up and (ii)with the MP512T face-down. In addition, the transmission factors for the MP512T and the printed circuit board were only evaluated using a Farmer IC.

Results: For all D_{sd} and all field sizes, the MP512T led to the surface dose increasing by less than 25% when in the beam. For D_{sd} >18cm the surface dose increase is less than 5%, and negligible for field size 5x5cm^2. The difference in the surface dose perturbation for the MP512T operating face up or operating face down is negligible (<2%) for all field sizes. The transmission factor of the MP512T ranged from 1.020 to 0.9950 for all measured D_{sd} and field sizes.

Conclusion: The study demonstrated that positioning the MP512T in air between the Linac head and the phantom produced negligible perturbation of the surface dose for D_{sd}>18cm, and was completely transparent for 6MV photon beams.

1. Introduction

Advanced treatment techniques such as Stereotactic Radiosurgery (SRS) and Stereotactic Body Radiation Therapy (SBRT), have been increasingly used for cancer treatments [1]. Generally, these techniques use a small field (less than 4 x 4 cm^2) to deliver a very highly conformed radiation dose to the target volume in a few fractions [2]. An important feature is a reduction of the radiation field to a sub-centimeter size for conformal tumor painting, and this can lead to electronic disequilibrium conditions which increase the uncertainties in dose calculations and measurements [3].

Due to the complexity of the SRS and SBRT delivery, a patient specific QA is needed to ensure that the delivered dose matches the planned dose distribution [4], [5]. Many devices have been developed for pre-treatment treatment verification [6]–[11] however, there is a considerable demand for real-time dose delivery verification. Such QA technology enables a real-time detection of major errors in the delivered dose [12].

The real time verification can be carried out by using a transmission-type detector positioned in the photon beam between the Linac head and the patient, or by means of an electronic portal imaging device (EPID) during the treatment [13]. The available commercial transmission detectors such as Dolphin (IBA Dosimetry, Germany) and David (PTW-Freiburg, Germany) are based on string ionization chambers and demonstrated good performance. However, their large pixel size and poor spatial resolution limit their effectiveness for SRS and SBRT with small

fields. Additionally, the increase in surface dose is one of the limitations of the transmission-type detectors for in-field measurements. Venkataraman *et al.* [14] showed an increase in the surface dose of about 44 % for a 20 x 20 cm^2 field and 70cm source to surface distance (SSD), and a mean transmission factor (TF) value of 0.967 with the Compass detector for in-field measurement and a 6 MV photon beam. The surface dose was also shown to decrease as the field size was decreased and SSD increased. The occurrence of these effects is due to an increase in electron contamination. Poppe *et al.* [15] stated that the DAVID dosimetry system also presented beam attenuation with attenuation factors of 0.953 ± 0.001 and 0.968 ± 0.001 for 6 MV and 15 MV respectively. Similar studies examining the percentage depth dose (PDD) including the surface dose region, demonstrated beam perturbation induced by the transmission-type detector [16]–[18]. Casar *et al.* [19] studied the influence of the Integral Quality Monitor (IQM) transmission detector based on wedge type integral over field response ionization chamber and reported that the effects of the IQM detector on photon beam properties were found to be small yet statistically significant. The Delta^4 (ScandiDos) detector, based on 2D diode array, has been introduced as an integrated transmission detector [20]. Li *et al.* [21] reported that the increase in surface dose of this system was about 1% - 9%.

Although some transmission QA dosimetry devices are available, the spatial resolution and beam perturbation for some of them make their use in the clinical practice for SRS and SBRT for real-time treatment verification questionable.

The 2D diode array Magic Plate 121 (MP121), developed at the Center for Medical Radiation Physics (CMRP), is based on small, single epi-diodes embedded in a KAPTON carrier with a 1cm pitch and overall thickness of only 0.45 mm [22]. Alrowaili *et al.* [23] explored the performance of MP121 operating in transmission mode in which the detector was mounted on

the head of a Linac. The MP121 demonstrated minimal beam perturbation leading to an increase in the surface dose of less than 0.5%, and a TF of about 0.98 for 6 MV, 10 MV and 18 MV photon fields. However, the spatial resolution of the MP121 detector limits its effectiveness in small field treatments in SRS and SBRT.

A new family of monolithic silicon detectors, the Magic Plate 512T (MP512T) and MP1024T, have been developed to fill the above gap in transmission detector technology and subsequent dose reconstruction. *In-phantom* dose measurements for SRS and SBRT QA [24]–[26] using the MP512T detector have been previously reported.

The thin transmission monolithic silicon detector is designed to be placed between the patient and the Linac head. Figure 1 shows a concept of the transmission monolithic silicon detector providing flexible spatial resolution by changing D_{sd}. Moving the detector along the beam axis between the patient surface and the Linac head enables the effective spatial resolution of the detector monitoring the radiation field to change due to the beam divergence. With small sized tumors, placement of the detector closer to the patient improves its effective spatial resolution.

The proposed movable transmission, highly effective spatial resolution silicon monolithic detector has another advantage in comparison with the currently used transmission detectors mounted on the Linac head. By moving the detector below the Linac head, the contribution of electrons scattered from the head of the Linac on the response of the detector is minimized, and the detector response is mostly driven by the photon energy fluence, which should simplify the 3D dose reconstruction algorithm.

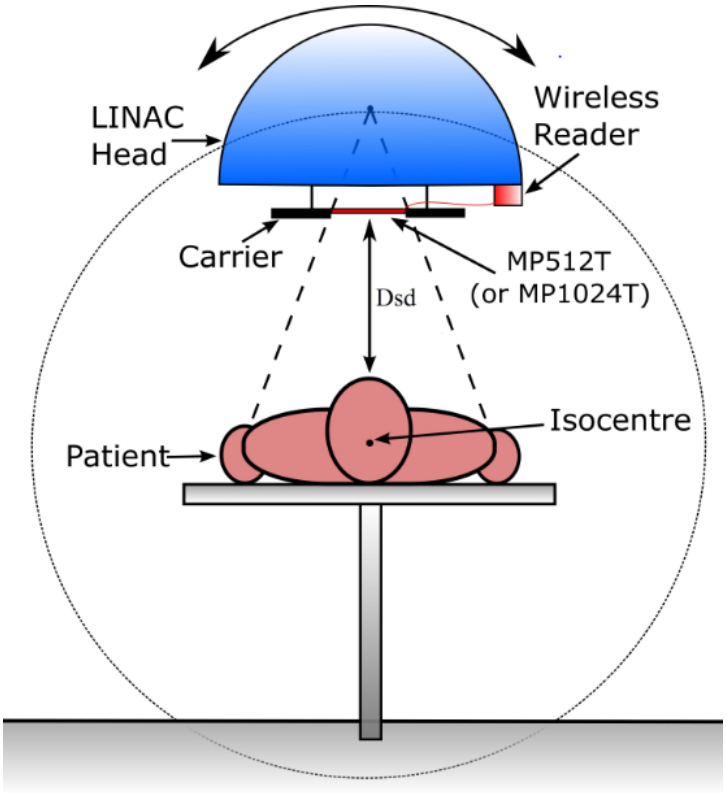

Figure 1: Concept of movable high-resolution transmission monolithic detector for dose reconstruction with variable spatial resolution.

While transmission and perturbation properties of the MP121 detector have been investigated in MV x-ray field, its design is essentially different from the monolithic MP512T detector. Taking into account that the MP512T can be placed very close to the patient, there can be differences with regard to increased skin dose and beam perturbation effects.

The purpose of this study is to investigate the influence on the treatment beam characteristics of the MP512T operating in transmission mode. We want to quantify perturbation, in particular, on the surface dose and beam transmission as a function of the treatment field size and the position the MP512T detector as the function of the detector-phantom distance.

2. Materials and Methods

2.1 Magic Plate 512 detector array and the movable stand

The MP512T is a monolithic p-type silicon diode array and is shown in Figure 2. It includes 512 pixels, each 0.5 x 0.5 mm^2 with a pixel pitch of 2 mm. The active area of the 2D array is 52 x 52 mm^2**.** The detector is wire bonded to a tissue equivalent PCB which is 0.5 mm thick. The detector is also covered by a layer of resin to avoid accidental damage.

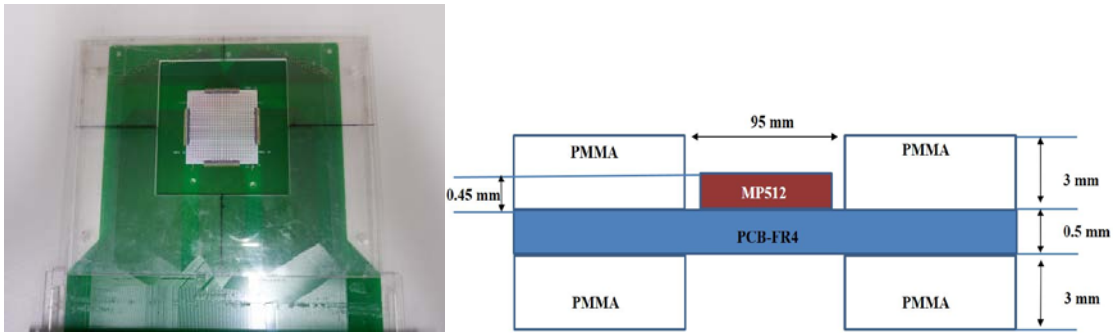

(a) (b)

Figure 2: (a) MP512T detector wire bonded to the PCB and sandwiched with the two PMMA slabs with an opening in place of the detector, (b) simplified schematic of MP512T packaging.

In this study, the MP512T array is sandwiched between 3 mm thick Poly Methyl Meth Acrylate (PMMA) sheets with a 95mm x 95 mm opening at the center of the board, as shown in Figure 2. In order for the MP512T to be positioned at any distance between the Linac head and the phantom surface, the detector was fixed on a movable stand made from PMMA plastic.

Figure 3 shows the MP512T placed on the movable stand. The holder is capable of precisely moving the detector along the beam axis (vertical direction in Figure 3).

(a)

(b)

Figure 3: The measurement setup with and without MP512T in a beam.

The effect of the MP512T detector on the surface dose and the TF were investigated as a function of field size and distance above the solid water phantom surface. The radiation field size is defined at a 100 cm SSD. Thus, the effective irradiation field size at the MP512T position depends on the distance from the solid water phantom, and ranged from about 2cm x 2 cm to 6cm x 6 cm at Linac head placement. The results will also be applicable to the MP1024T due to

the fact that the detector size is the only difference between the MP512T and MP1024T detector arrays. The MP1024T has 976 pixels (0.25mm x 0.25 mm each) and 1 mm pitch in the central area of the detector (20x20 mm^2) and, a 2 mm pitch outside the central area and a detector size of 65 mm x 65 mm.

2.2 Surface dose measurement

To measure the surface dose, a Markus ionization chamber (IC) (PTW, Freiburg, Germany, model N23343) was positioned at the surface of the solid water phantom at central axis (CAX) corresponding to isocenter, with 100 cm SSD. The back scattering solid water phantom was 10 cm thick. The IC was read out by a PTW UNIDOS model T10002-20713 electrometer. All readings from the Markus IC have been corrected for over response by using the correction factor given by Chen *et al.* [27].

2.2.1 The influence of MP512T on the surface dose

The perturbation of the surface dose was reported as a percentage difference between the surface doses measured with and without the MP512T in position. Both the MP512T detector and the Markus IC were aligned at the center of the beam axis. All measurements were performed using a 6 MV photon beam from a Varian linear accelerator (Model 21 iX). For each measurement, 200 monitor units (MUs) were delivered. The MP512T distance from the solid water phantom surface was varied from 0.3 cm to 24 cm. The measurements were carried out for irradiation field sizes (IFS) of 5 x 5 cm^2, 8 x 8 cm^2 and 10 x 10 cm^2 with the MLC matching the Linac jaws. To examine the reproducibility of the Markus IC, the readings were acquired at least three times

under the same conditions. The detector measurement uncertainty was found to be ± 0.2% (1 standard deviation).

The influence of the MP512T on the surface dose when placed the detector face-up and face-down at different D_{sd} was evaluated. The set of measurements, as above, were repeated. Figure 4 shows the schematic of the surface dose measurement setup with MP512T in a beam (a) face-up; (b) face-down. For each position and field size, the readings were obtained at least three times, and the average was calculated.

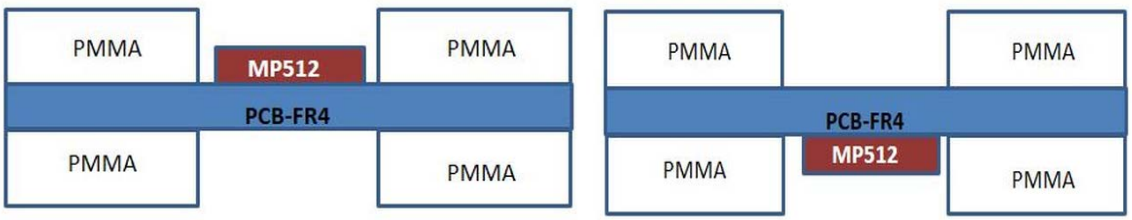

(a) (b)

Figure 4: Schematic of MP512T (a) face up and (b) face down.

2.2.2 Effect of Printed Circuit Board on MP512T surface dose measurement

To evaluate the effect of only the 0.5 mm thick PCB on the surface dose, the PCB without the silicon detector was placed on the movable stand. The surface dose measurements were performed using the Markus IC in a solid water phantom for open field and the PCB in the beam similar as described in 2.2.1.

2.3 The transmission factor measurement

The TF of the MP512T detector and the PCB were investigated by measuring the ratio of the doses at d_{max} with and without the MP512T detector in a beam for radiation field sizes of 5x5 cm^2, 8x8 cm^2 and 10x10 cm^2, and SSD of 100 cm for a 6 MV photon beam. The MP512T detector was placed in the beam at various D_{sd} ranging from 0.3 cm to 24 cm. A Farmer IC (Model 2571A) was used for dose measurements. The same set up was repeated at a depth of 10 cm and a source axial distance (SAD) of 100 cm for a 6 MV photon beam.

3. Results

3.1 Surface dose measurement

3.1.1 The effect of the MP512T detector on surface dose measurement

Figure 5 shows the percentage difference of surface dose with and without the MP512T detector in the beam path, as a function of field size and distance from the solid water phantom surface. The maximum difference in surface dose was nearly 30%, and this was found at the distance of 0.3 cm, particularly in the large 10 x 10 cm^2 field. The difference in surface dose decreased as the distance of MP512T from the solid water phantom surface increased. At D_{sd} >18 cm, the difference was less than 5% for all IFSs. At the small field size of 5 x 5 cm^2, the percentage difference was within ±1 % (1 standard deviation).

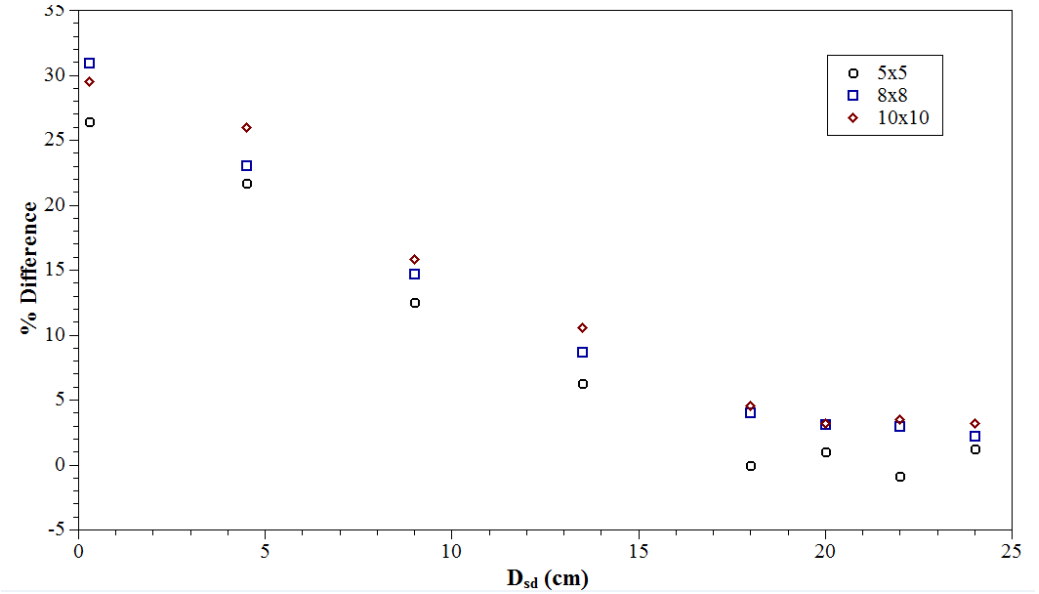

Figure 5: The percentage difference of surface dose with and without MP512T in a beam as a function of distance of the MP512T from the phantom surface and field size for a 6 MV photon beam.

Figure 6 shows the percentage difference of surface dose between the two MP512T detector orientations (ie face-up or face-down) at various distances from the phantom surface and different IFSs. The difference was within 2.5 % (1 standard deviation) for all distances and field sizes.

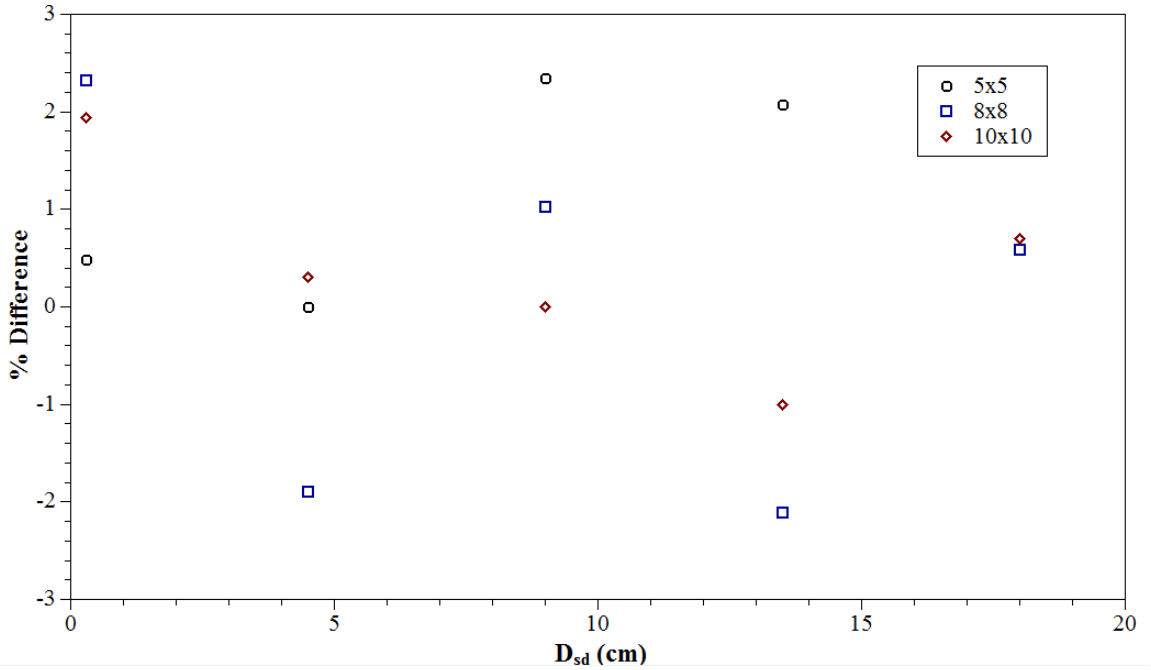

Figure 6: The percentage difference of surface dose when MP512T is face-up and face-down in the beam as a function of distance from the phantom surface and field size for a 6MV photon beam.

3.2.2 Effect of Printed Circuit Board on surface dose measurement

Figure 7 shows the percentage difference of the surface dose measured with and without the PCB in the beam. Similarly, to Figure 5, the surface dose difference increased when the PCB was closer to the phantom surface. At PCB distances of more than 18 cm, the percentage difference is close to zero for all IFSs. At a PCB distance of 0.3 cm, the surface dose increased by about 15% (1 standard deviation) for all IFSs.

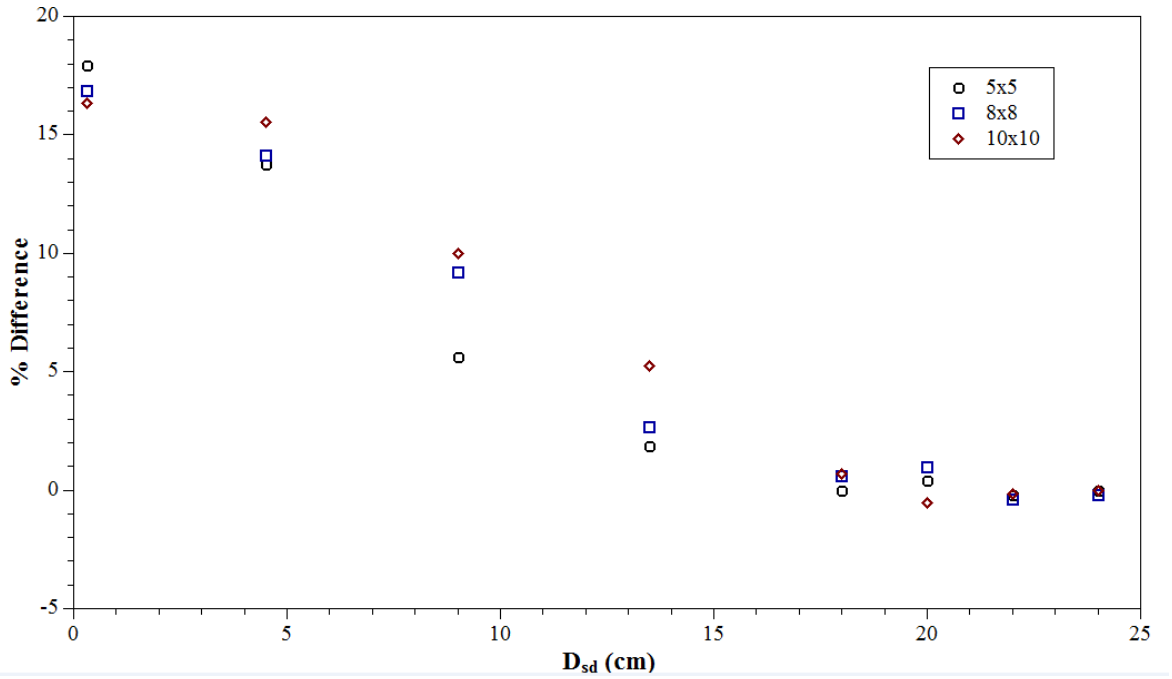

Figure 7: The percentage difference of the surface dose with and without the PCB in a beam as a function of distances of MP512T from the phantom surface and field size for 6 MV photon beam.

3.2 The transmission factor measurement

At a depth of d_{max}, the relative dose difference increases slightly as the distance between the phantom surface and MP512T (or blank PCB) decreases from 18 cm to 0.3 cm. For D_{sd} < 18cm, the TF changes about 1.5-2.0 % (1 standard deviation) and 0.5% (1 standard deviation) for the MP512T detector and PCB respectively, for all IFSs and all distances above 18 cm, is close to 1. These results are presented in Table 1 Similar behavior of the transmission factor is observed at a depth of 10 cm as shown in Table 2.

Table 1. Measured TF at d_{max} for 6 MV photon beam, SSD =100 cm. The TF is presented separately for various distances and IFSs for MP512T and the PCB

D_{sd} (cm)	MP512T			PCB		
	5x5 cm^2	8x8 cm^2	10x10 cm^2	5x5 cm^2	8x8 cm^2	10x10 cm^2
0.30	1.0130	1.0151	1.0198	1.0055	1.0058	1.0067
4.50	1.0120	1.0141	1.0186	1.0051	1.0054	1.0062
9.00	1.0096	1.0104	1.0133	1.0032	1.0038	1.0046
13.50	1.0040	1.0047	1.0069	1.0018	1.0026	1.0029
18.00	0.9985	0.9993	0.9996	0.9980	0.9982	0.9989
20.00	0.9981	0.9990	0.9988	0.9978	0.9982	0.9990
22.00	0.9975	0.9977	0.9991	0.9980	0.9980	0.9980
24.00	0.9971	0.9980	0.9985	0.9976	0.9975	0.9973

Table 2. Measured TF at depth of 10 cm for 6 MV photon beam, SAD =100 cm. The TF is presented separately for various distances and IFSs for MP512T and the PCB

D_{sd} (cm)	MP512T			PCB		
	5x5 cm^2	8x8 cm^2	10x10 cm^2	5x5 cm^2	8x8 cm^2	10x10 cm^2
0.30	1.0190	1.0200	1.0220	1.0122	1.0129	1.0137
4.50	1.0182	1.0190	1.0216	1.0120	1.0124	1.0131
9.00	1.0132	1.0147	1.0159	1.0085	1.0099	1.0105
13.50	1.0069	1.0076	1.0092	1.0059	1.0063	1.0062
18.00	1.0022	1.0032	1.0037	1.0018	1.0024	1.0030
20.00	1.0020	1.0022	1.0020	1.0012	1.0019	1.0020
22.00	1.0010	1.0012	1.0015	0.9991	0.9993	0.9994
24.00	0.9993	0.9997	1.0011	0.9991	0.9989	0.9992

4. Discussion

The QA in SRS and SBRT is complicated because of small field delivery using IMRT or VMAT for SBRT, and high definition MLCs and small cones for SRS. Thus, the treatment verification requires high spatial resolution QA tools, which accurately provide the relevant dose information in real-time during the treatment delivery for each gantry angle, followed by 3D dose reconstruction after full treatment plan delivery. The new QA devices, the monolithic silicon pixelated detectors MP512T and MP1024T, were introduced, while experimental results were presented for the MP512T detector only because of the similarity of the device layout. The MP512T and MP1024T detectors will provide variable, yet high effective spatial resolution when placed at different positions in the beam between the Linac head and the patient, in such a

way that attenuation by the PMMA frame (Figure 1) is avoided by ensuring beam projection at any depth is within the area of silicon detector or PCB. These detectors allow us to obtain a variably effective spatial resolution from 2 mm to 4 mm for the MP512T detector and from 1 mm to 4 mm for the MP1024T, depending on the position of the detector on the beam axis relative to the Linac head. Another advantage of this approach is the reduction in the contribution of scattered electrons from the Linac head to the response of the transmission detectors. The thin 0.45 mm silicon substrate and 0.5 mm PCB produce minimal beam perturbation.

It was demonstrated that the MP512T and the PCB both increase the surface dose due to Compton electrons originating from the silicon and the PCB. The partial contribution of the PCB alone led to the rise in the surface dose of about 60% compared to the increase in the surface dose from the MP512T detector (Figure 5 and Figure 7). Taking into account that Compton electrons, in this case, are mostly of MeV energy range, it suggests that an opening or recess in the PCB under the silicon monolithic detector active area is recommended to further reduce the skin dose excess for all considered IFSs. We also demonstrated only a 2% difference in the excess surface dose between the MP512T detector face-up and face-down orientations (Figure 6), and will be close to zero if an opening or recess is introduced in the PCB substrate. A thin light protective coating should be introduced above the silicon detector to avoid stray light influencing the detector response. It can easily be achieved by adding black filler to the thin layer of resin protecting the silicon detector.

The transmission coefficient of the MP512T detector measured at d_{max} is close to 1 with a deviation of about 1.010-1.020 as the distance between the MP512T detector and the phantom surface decreased below 18 cm. Providing an opening in the PCB under the silicon monolithic

detector will make the transmission coefficient closer to 1 for any placement of the proposed transmission detectors between patient and Linac head.

Mechanical realization of the proposed transmission detector in a clinical scenario is still to be done, but is straight forward and will be realized on a telescopic jig attached to the Linac head block tray slot together with a wireless reader developed at CMRP similar to other transmission detectors described above.

5. Conclusion

The new transmission monolithic detectors MP512T and MP1024T for small radiation fields with a variable effective spatial resolution of up to 1 mm at differing positions between the Linac head and the patient for real time QA for SRS and SBRT have been introduced. The MP512T is characterized and demonstrated minimal skin dose increase and dose perturbation at d_{max}. The effective spatial resolution in the dosimetry of the small photon beams can be improved by moving the MP512T detector along the beam axis, with the best spatial resolution reported when the detector is closest to the surface of the phantom. Reduction of the measured skin dose excess can be achieved by reducing the silicon substrate thickness to 0.3mm and having a recession in a packaging of the detector [22] on the PCB with a recess to accommodate the silicon detector. Future work will be directed to the development of a 3D dose reconstruction algorithm in a phantom, based on the MP512T detector response at different detector positions between the Linac and phantom surface.

Acknowledgement

Kananan Utitsarn was supported by Lopburi Cancer Hospital Department of Medical Service, Ministry of Public Health Thailand. The authors would like to acknowledge the National Health and Medical Research Council of Australia which funded this project. The project Grant No. is APP1030159.

Reference

[1] L. Potters *et al.*, "American Society for Therapeutic Radiology and Oncology and American College of Radiology Practice Guideline for the Performance of Stereotactic Body Radiation Therapy," *Int. J. Radiat. Oncol. Biol. Phys.*, vol. 60, no. 4, pp. 1026–1032, 2004.

[2] S. K. Seung *et al.*, "American College of Radiology (ACR) and American Society for Radiation Oncology (ASTRO) practice guideline for the performance of stereotactic radiosurgery (SRS)," *Am. J. Clin. Oncol.*, vol. 36, no. 3, p. 310, 2013.

[3] I. J. Das, G. X. Ding, and A. Ahnesjö, "Small fields: nonequilibrium radiation dosimetry.," *Med. Phys.*, vol. 35, no. 1, pp. 206–215, 2008.

[4] J. M. Galvin and G. Bednarz, "Quality assurance procedures for stereotactic body radiation therapy," *Int. J. Radiat. Oncol. Biol. Phys.*, vol. 71, no. 1, pp. S122–S125, 2008.

[5] E. E. Klein *et al.*, "Task Group 142 report: quality assurance of medical accelerators," *Med. Phys.*, vol. 36, no. 9, pp. 4197–4212, 2009.

[6] B. Poppe *et al.*, "On the resolution and the sensitivity of 2-dimensional ionization chamber array (PTW Type 10024)," *Z Med Phys*, vol. 4, pp. 287–291, 2005.

[7] B. Poppe *et al.*, "Two-dimensional ionization chamber arrays for IMRT plan verification," *Med. Phys.*, vol. 33, no. 4, pp. 1005–1015, 2006.

[8] R. J. Watts, "Evaluation of a diode detector array for use as a linear accelerator QC

device," *Med. Phys.*, vol. 25, no. 2, pp. 247–250, 1998.

[9] D. Létourneau, M. Gulam, D. Yan, M. Oldham, and J. W. Wong, "Evaluation of a 2D diode array for IMRT quality assurance," *Radiother. Oncol.*, vol. 70, no. 2, pp. 199–206, 2004.

[10] P. a Jursinic and B. E. Nelms, "A 2-D diode array and analysis software for verification of intensity modulated radiation therapy delivery.," *Med. Phys.*, vol. 30, no. 5, pp. 870–879, 2003.

[11] M.-H. Lin, I. Veltchev, S. Koren, C. Ma, and J. Li, "Robotic radiosurgery system patient-specific QA for extracranial treatments using the planar ion chamber array and the cylindrical diode array," *J. Appl. Clin. Med. Phys.*, vol. 16, no. 4, 2015.

[12] B. Mijnheer, S. Beddar, J. Izewska, and C. Reft, "In vivo dosimetry in external beam radiotherapy," *Med. Phys.*, vol. 40, no. 7, 2013.

[13] L. N. McDermott, M. Wendling, J.-J. Sonke, M. van Herk, and B. J. Mijnheer, "Replacing pretreatment verification with in vivo EPID dosimetry for prostate IMRT," *Int. J. Radiat. Oncol. Biol. Phys.*, vol. 67, no. 5, pp. 1568–1577, 2007.

[14] S. Venkataraman, K. E. Malkoske, M. Jensen, K. D. Nakonechny, G. Asuni, and B. M. C. McCurdy, "The influence of a novel transmission detector on 6 MV x-ray beam characteristics," *Phys. Med. Biol.*, vol. 54, no. 10, pp. 3173–3183, 2009.

[15] B. Poppe *et al.*, "DAVID--a translucent multi-wire transmission ionization chamber for in vivo verification of IMRT and conformal irradiation techniques," *Phys. Med. Biol.*, vol. 51, no. 5, pp. 1237–1248, 2006.

[16] M. K. Islam *et al.*, "An integral quality monitoring system for real-time verification of intensity modulated radiation therapy," *Med Phys*, vol. 36, no. 12, pp. 5420–5428, 2009.

[17] Y. Nakaguchi, F. Araki, M. Maruyama, and S. Saiga, “Dose verification of IMRT by use of a COMPASS transmission detector,” *Radiol. Phys. Technol.*, vol. 5, no. 1, pp. 63–70, 2012.

[18] J. Thoelking, Y. Sekar, J. Fleckenstein, F. Lohr, F. Wenz, and H. Wertz, “Characterization of a new transmission detector for patient individualized online plan verification and its influence on 6MV X-ray beam characteristics,” *Z. Med. Phys.*, vol. 26, no. 3, pp. 200–208, 2016.

[19] B. Casar *et al.*, “Influence of the Integral Quality Monitor transmission detector on high energy photon beams: A multi-centre study,” *Z. Med. Phys.*, 2017.

[20] D. Hoffman, E. Chung, C. Hess, R. Stern, and S. Benedict, “SU-E-T-571: Newly Emerging Integrated Transmission Detector Systems Provide Online Quality Assurance of External Beam Radiation Therapy,” *Med. Phys.*, vol. 42, no. 6, p. 3467, 2015.

[21] T. Li, Q. J. Wu, T. Matzen, F.-F. Yin, and J. C. O’Daniel, “Diode-based transmission detector for IMRT delivery monitoring: a validation study,” *J. Appl. Clin. Med. Phys.*, vol. 17, no. 5, 2016.

[22] J. H. D. Wong *et al.*, “Characterization of a novel two dimensional diode array the ‘magic plate’ as a radiation detector for radiation therapy treatment,” *Med. Phys.*, vol. 39, no. 5, pp. 2544–2558, 2012.

[23] Z. A. Alrowaili, M. L. F. Lerch, M. Petasecca, M. G. Carolan, P. E. Metcalfe, and A. B. Rosenfeld, “Beam perturbation characteristics of a 2D transmission silicon diode array , Magic Plate,” *J. Appl. Clin. Med. Phys.*, vol. 17, no. 2, pp. 85–98, 2016.

[24] A H. Aldosari *et al.*, “A two dimensional silicon detectors array for quality assurance in stereotactic radiotherapy: MagicPlate-512.,” *Med. Phys.*, vol. 41, no. 9, p. 91707, 2014.

[25] N. Stansook *et al.*, “Technical Note: Angular dependence of a 2D monolithic silicon diode array for small field dosimetry,” *Med. Phys.*, vol. 44, no. 8,pp. 4313-4321,2017.

[26] K. Utitsarn *et al.*, “Optimisation of output factor measurements using the Magic Plate 512 silicon dosimeter array in small megavoltage photon fields,” *J. Phys. Conf. Ser.*, vol. 777, no. 1, 2017.

[27] F. Q. Chen, R. Gupta, and P. Metcalfe, “Intensity modulated radiation therapy (IMRT) surface dose measurements using a PTW advanced Markus chamber,” *Australas. Phys. Eng. Sci. Med.*, vol. 33, no. 1, pp. 23–34, 2010.